Available online at www.sciencedirect.com
ScienceDirect
Thermochimica Acta 471 (2008) 61–69
thermochimica acta
www.elsevier.com/locate/tca

Thermal behavior of cellulose acetate produced from homogeneous acetylation of bacterial cellulose

Hernane S. Barud [a,*], Adalberto M. de Araújo Júnior [a], Daniele B. Santos [a], Rosana M.N. de Assunção [b], Carla S. Meireles [b], Daniel A. Cerqueira [b], Guimes Rodrigues Filho [b], Clóvis A. Ribeiro [a], Younes Messaddeq [a], Sidney J.L. Ribeiro [a]

[a] *State University of São Paulo (UNESP), Institute of chemistry, Department of Inorganic and General Chemistry, R: Francisco Degni, s/n, P.O. Box 355, 14801-970 Araraquara, SP, Brazil*
[b] *Federal University of Uberlândia, Institute of Chemistry, Av. João Naves de Avila 2121, P.O. Box 593, 38400-902 Uberlândia, MG, Brazil*

Received 31 May 2007; received in revised form 6 February 2008; accepted 12 February 2008
Available online 17 February 2008

Abstract

Cellulose acetate (CA) is one of the most important cellulose derivatives and its main applications are its use in membranes, films, fibers, plastics and filters. CAs are produced from cellulose sources such as: cotton, sugar cane bagasse, wood and others. One promissory source of cellulose is bacterial cellulose (BC). In this work, CA was produced from the homogeneous acetylation reaction of bacterial cellulose. Degree of substitution (DS) values can be controlled by the acetylation time. The characterization of CA samples showed the formation of a heterogeneous structure for CA samples submitted to a short acetylation time. A more homogeneous structure was produced for samples prepared with a long acetylation time. This fact changes the thermal behavior of the CA samples. Thermal characterization revealed that samples submitted to longer acetylation times display higher crystallinity and thermal stability than samples submitted to a short acetylation time. The observation of these characteristics is important for the production of cellulose acetate from this alternative source.

Keywords: Bacterial cellulose; Homogeneous acetylation; Cellulose acetate; Thermal properties

1. Introduction

Cellulose acetate (CA) is one of the most important cellulose derivatives and its main applications are in membranes, films, fibers, plastics, filters, and so on [1]. Generally, CAs are produced from homogeneous or heterogeneous processes from innumerous cellulose sources such as: cotton, sugar cane bagasse, wood and others [2]. In this sense, one promissory source of cellulose is bacterial cellulose (BC). BC is produced by Gram-negative acetic acid bacteria *Acetobacter xylinum* (or reclassified *Gluconoacetobacter xylinus*) and displays several unique properties when compared to plant cellulose. It is produced as highly hydrated membranes free of lignin and hemicelluloses and it has a higher molecular weight and higher crystallinity in an ultrafine reticulated structure. A multitude of applications is proposed in industry (paper, textile and food) and as a biomaterial in cosmetics and medicine as a consequence of its special properties [3].

Few studies have reported on the production of CAs via bacterial cellulose acetylation [4–6]. These works have focused on the acetylation process and the physical properties of the derivatives.

The acetylation process depends on the accessibility of cellulose fibers and the susceptibility of individual cellulose crystallites. For production of cellulose acetate, the homogeneous process was used. In the homogeneous process, where there is non swelling agent, cellulose triacetate (CTA) is solubilized in the reaction medium as it is produced. The control

* Corresponding author. Tel.: +55 16 33016600; fax: +55 16 33016636.
E-mail addresses: hsbarud@iq.unesp.br, hernane.barud@gmail.com (H.S. Barud).

0040-6031/$ – see front matter © 2008 Elsevier B.V. All rights reserved.
doi:10.1016/j.tca.2008.02.009

of the acetylation time can be an important aspect to the variable degree of acetylation and cellulose acetate's physical structure.

For this paper, cellulose acetate was produced from bacterial cellulose using homogeneous acetylation. The chemical modification was observed as a function of acetylation time and characterized by Fourier Transform Infrared Spectroscopy (FTIR) and solid state ^{13}C nuclear magnetic resonance (NMR). The thermal behaviors of the materials were evaluated by thermogravimetric analysis (TG) and differential scanning calorimetry (DSC). Changes in the physical properties were observed using scanning electronic microscopy (SEM), transition electron microscopy (TEM) and X-ray diffraction.

2. Experimental

2.1. Acetylation of cellulose acetate

Bacterial cellulose membranes were supplied from Fibrocel-Produtos Biotecnológicos LTDA, Ibiporã, Brazil. The DP of bacterial cellulose was determinate via intrinsic viscosity measurements. The bacterial cellulose showed a DP of 900.

30 cm × 50 cm, 1.5 thick, hydrated bacterial cellulose membranes were dried at 105 °C. Cellulose acetate was produced from the homogeneous acetylation reaction of bacterial cellulose as described by Sassi and Chanzy [7]. Dried cellulose, acetic acid, anhydride acetic and sulfuric acid as catalyst were mixed. During the reaction, the cellulose was modified and a soluble product, the CA, was obtained in the reaction medium. Cellulose acetate was obtained by precipitation with the addition of water to the mixture, being separated by filtration and washed with water.

2.2. Degree of substitution (DS)

The chemical degree of substitution (DS) of the BC acetylated samples was determined using saponification reaction [2].

2.3. FTIR characterization of bacterial cellulose and cellulose acetate

FTIR spectra were obtained with dried powdered samples on a PerkinElmer Spectrum 1000 Fourier Transform Infrared Spectrophotometer. Pellets were prepared from mixtures of the samples and KBr (1:100 in weight). Twenty-eight scans were accumulated at a resolution of 4 cm^{-1}.

2.4. ^{13}C-CPMAS-NMR spectroscopy

High-resolution ^{13}C-CPMAS-NMR spectra of BC and cellulose acetate samples were measured in a magnetic field of 7.04 T with a spectrometer, model Varian Unity INOVA probe CPMAS 7 mm. Measurements were carried out at a spin of 4.5 kHz, frequency ^{13}C 75.43 MHz, contact time 0.7 ms, with $\pi/2$ pulses (4 μs length) and recycle delays of 1 s.

2.5. WAXD characterization

X-rays diffraction patterns were obtained using a Kristalloflex Simens Diffractometer with a Ni filter and Cu Kα radiation from 4° to 70°.

2.6. Thermal behavior

2.6.1. TG curves

TG curves were obtained from SDT equipment from TA Instruments. The conditions used in the experiments were: nitrogen atmosphere at a flow rate of 50 mL min^{-1}, heating rate of 10 °C min^{-1} from 10° to 600 °C and alumina pans.

2.6.2. DSC curves

DSC curves were obtained from ambient temperature to 400 °C from DSC equipment, model Q600 from TA Instruments using a sealed aluminum pan under a nitrogen atmosphere (50 mL min^{-1}) and a heating rate of 10 °C min^{-1}. The instrument was calibrated (temperature and enthalpy) using the indium standard.

2.7. SEM characterization of the samples

A scanning electron microscopy image was obtained from a FEG-SEM JSM 6330F at the LNLS (Brazilian Synchroton Light Laboratory). Samples were coated with a 3 nm thick carbon layer.

2.8. TEM characterization of the samples

Transmission electron microscopy images were obtained from a Philips CM2. The CA samples were dissolved in an ethanol solution. Suspensions were put in a cooper support.

3. Results and discussion

Results for degrees of substitution of BC acetylated at different times are presented in Fig. 1. From 0.5 h to 24 h of reaction, the DS values vary from 2.30 to 2.77. There is a relation between the DS value and the properties of the polymer. One of these

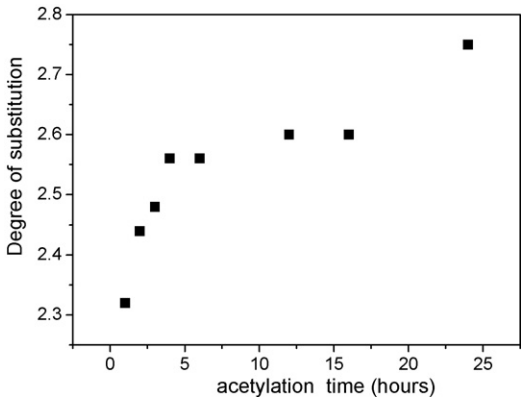

Fig. 1. Chemical DS of cellulose acetate as a function of the acetylation time.

properties is biodegradation. According Samios et al. [8] and Gross and Kalr [9], in general, low DS values leading product with more potential for biodegradation. The control of the DS values is interesting since properties like the rate of biodegradation and solubility of acetylated cellulose can be modified.

The DS values increase in the first hours of acetylation (0.5–4 h). Under the conditions of the synthesis used in this work and in the initial stage of the process (0.5 h), cellulose diacetate (DS 2.30) was produced. After 4 h of reaction, the DS is quite constant until 16 h of reaction and a structure close to cellulose triacetate was produced. In this case, the accessibility of hydroxyl groups in the modified cellulose is more difficult and the modification in the DS value only occurs at 24 h of reaction where the DS value reached was 2.77.

Fig. 2 shows the FTIR of bacterial cellulose and acetylated samples. The modification of the CA spectra can be observed for the whole acetylation time range, from 0.5 h to 24 h.

CA formation can be monitored by the absorption band at 1755 cm^{-1} assigned to C=O ester stretching, plus the 1237 cm^{-1} band assigned to stretching of C–O of the acetyl group and also the blue shift of 20 cm^{-1} observed for the band at 896 cm^{-1}, assigned to β glucosidic linkages between the sugar units (Table 1).

Another important aspect observed in the cellulose acetate spectrum is the decreasing absorption intensity of the band located at around 3400 cm^{-1} assigned to the stretching of the hydroxyl group when compared with bacterial cellulose. This decreasing occurs because the hydroxyl groups are substituted by acetyl groups in the reaction and the pattern of the cellulose acetate spectrum corroborates the DS value for a cellulose triacetate.

Samples submitted to a higher acetylation time presents lower intensity bands on the 3400 cm^{-1} characteristic of more acetylated materials. These results corroborate the chemical degree of substitution.

The ^{13}C-CPMAS-NMR spectra for BC and acetylated samples are shown in Fig. 3. In Table 2, the main resonance lines for BC and cellulose acetate are represented [10].

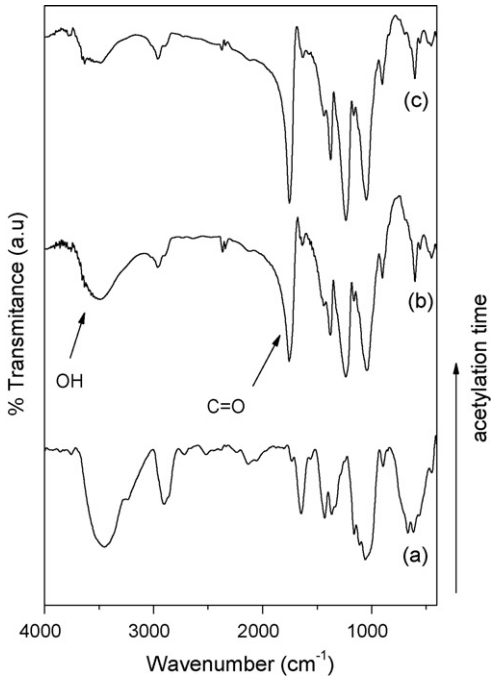

Fig. 2. FTIR spectra for bacterial cellulose (a), cellulose acetate 1 h (b), cellulose acetate 24 h (c).

Table 2
Resonance lines for bacterial cellulose and cellulose acetate

Samples	Assignments δ (ppm)					
	C=O	C1	C4	C2–C5	C6	C-Me
Bacterial cellulose		105	89.8	73.0, 72.0, 71.0	65.9	
Cellulose acetate	174	102	87.0	74.1[a]	62	21

[a] No well defined peaks.

The spectra for acetylated samples showed a set of peaks that confirms modification in the BC structure. The respective resonance lines for cellulose acetate are assigned to the CO (175 ppm), C1 (102 ppm), C6 (66 ppm) and CH_3 (21 ppm), and

Table 1
Assignments of main infrared absorption bands in cellulosic materials

Wave number (cm^{-1})		Assignment
Bacterial cellulose	Cellulose acetate	
	3643 (s)	OH stretching
3447 (s)	3479 (s)	
	2961	CH stretching of CH_2 and CH_3 groups
2904	2904	
1729 (w)		C=O stretching of acetyl or carboxylic acid
	1755 (s)	C=O stretching of ester
1647 (s)		H–O–H bending of absorbed water and/or C=O stretching of amid
	1648	H–O–H bending of absorbed water
1432	1444	CH_2 bending or OH in plane bending
1332	1374	C–H deformation (CH_3 or OH in plane bending)
	1237 (s)	C–O stretching of acetyl group
1168	1167	C–O–C antisymmetric bridge stretching
1041	1054	C–O symmetric stretching of primary alcohol
896	915	β glucosidic linkages between the sugar units

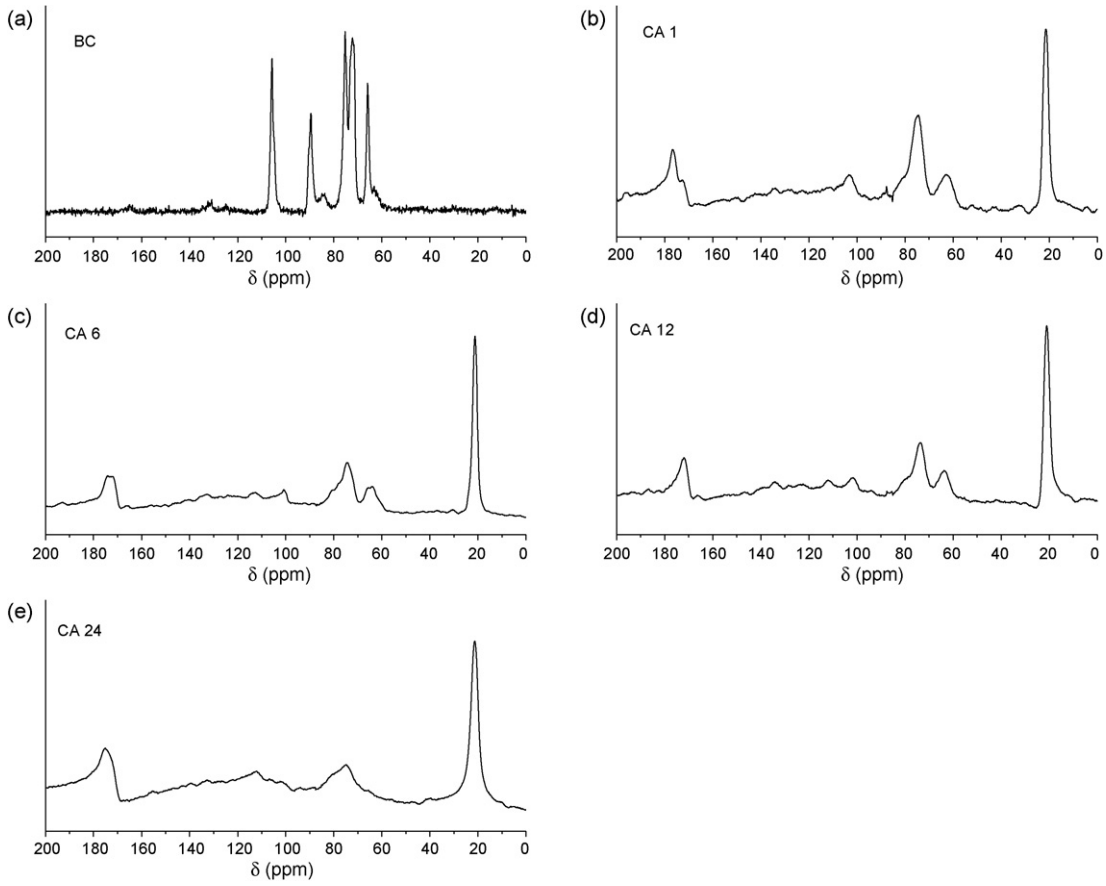

Fig. 3. Solid state ^{13}C-CPMAS-NMR spectra: (a) BC; (b) CA 1 h; (c) CA 6 h; (d) CA 12 h; (e) CA 24 h.

CH_3 carbons from the downfield side, except for a cluster of resonances at 70–84 ppm which belong to the C2–C5 [6,10,11].

The crystalline and disordered components were detected respectively as downfield and upfield lines for the C4 or C6 carbon [6]. As can be observed from the intensities of the C4 (89.8 ppm) and the C6 (66 ppm) resonance lines decreasing with increasing reaction time. The modifications and decreasing of the NMR spectra lines, particularly the lines related to C4 and C6, are an indication of chemical modification and changes in crystalline and amorphous components in the samples. The chances in these components are observed due to microfibrils modifications reached to an acetylated product less crystalline than unmodified cellulose.

The acetylation gradually modified the characteristic of the NMR spectra patterns. These modifications are associated to three factors: changes in the DS during the synthesis, the low homogeneity in the distribution of substitution groups and the crystalline structure.

The morphological changes of polymers can be followed via the evaluation of the XRD curves in Fig. 4 and the micrographs of scanning electronic microcopy as shown in Fig. 5. The XRD results presented in Fig. 4 allow us to analyze changes in the crystallinity of the samples after the synthesis.

Fig. 4 refers to the BC diffraction. Peaks localized at 15° and 22.5° are assigned to the cellulose 1α and 1β phases ($1\,0\,0_{1\alpha}$, $1\,1\,0_{1\beta}$ and $0\,1\,0_{1\beta}$ planes at 15° and $1\,1\,0_{1\alpha}$ and $2\,0\,0_{1\beta}$ at 22.5°) [12].

The other figures represent BC derivatives. Two main broad peaks located at around 8° and 20° are observed together with a set of ill resolved peaks at 13°, 17° and 21°.

The main peak located at approximately 8° is cited as the principal characteristic of semicrystalline acetylated derivative cellulose [2]. The position of this peak indicates the generation of a disorder when the cellulose was acetylated. This change in the WAXD pattern occurs during cellulose acetylation. The disorder is caused by the projection of the substituting groups (acetyl groups) along the axes and is associated with an increase in the interfibrillar distance and is also associated to the breakdown of microfibrilllar structures.

Cellulose acetate presents a low degree of crystallinity, this fact can be observed from the WAXD pattern. This reduction in crystallinity in relation to the original bacterial cellulose occurs due to the substitution of the hydroxyl groups by acetyl groups that have a greater volume.

A very important piece of information is that samples submitted to a long acetylation time (a greater DS) have a higher crystallinity than samples acetylated for a short time. It is suggested that the more uniform CAs were obtained due to better chain packing [2].

Fig. 5 shows selected TEM images of BC and acetylated samples.

Fig. 5a gives an overview of the dried bacterial cellulose. The SEM image shows the microfibrillar structure of cellulose, and aggregates of semicrystalline extended-cellulose

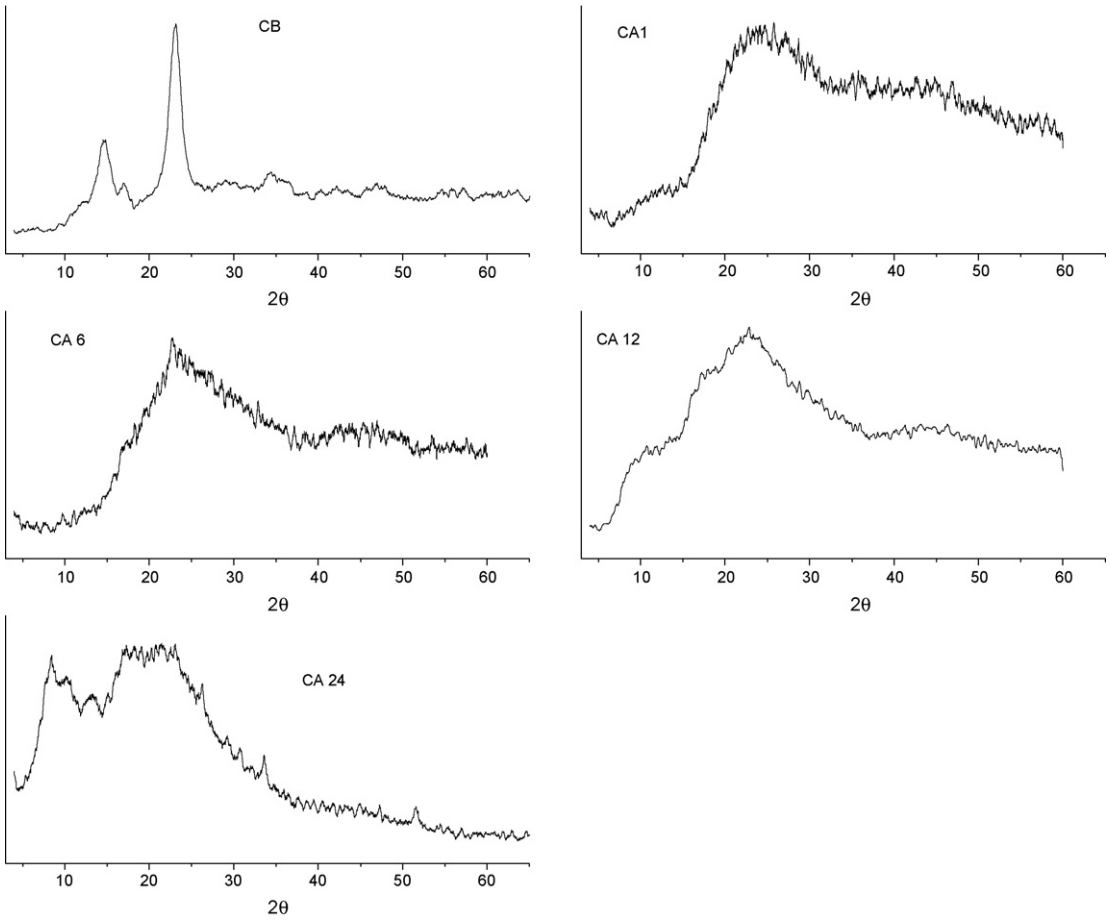

Fig. 4. XRD curves for bacterial cellulose and acetylated materials.

chains in an ultrafine network structure. This structure consists of continuous nano-fibers about 10 nm thick and 50 nm wide [13].

Cellulose fibers undergo substantial morphological changes as can be observed from the TEM micrographs. During acetylation process, the fibers undergo swelling and form a sponge-like structure. This process was more accentuated for CA produced at 24 h.

According to Sassi and Chanzy [7], the acetylation reaction seems to start within the amorphous region, and in a second step, the acetylation occurs in the crystallites as an erosion mechanism, with the acetylation beginning at the exterior of the crystallites and progressing toward their centre. The aspect presented for acetylated cellulose samples seems to point to the afore-mentioned mechanism. The increase in the acetylation time increases the fiber swelling and this fact may be a possible explanation of the CA's high DS when the sample is prepared in a 24-h reaction as verified via chemical DS data.

The CA produced from 24-h acetylation presents a more crystalline structure in accordance with the XRD data. This fact can be attributed to a more homogeneous distribution of the acetyl groups in the CTA produced with a high DS. This heterogeneous distribution led to the coexistence of unreached and preacetylated materials. In this condition, due to the low homogeneity of the system, the CA should present a low crystallinity.

The thermal properties of cellulose derivatives are sensitive to DS changes and to the uniformity of the substitution-group distribution. Fig. 6 shows the DSC curves for BC and CAs.

All curves have in common the presence of a broad endothermic event between ambient temperature (25 °C) and 100 °C. This event is attributed to water desorption from polysaccharide structure. The bacterial cellulose showed a broad endothermic peak at 285 °C that can be attributed to the thermal decomposition of the cellulose.

CA samples showed endothermic peaks in the range of 160–300 °C. The CA prepared from a 1-h reaction time showed an endothermic peak at 161 °C. This peak can be associated to the decomposition of the partly hydrolyzed cellulose. The acid treatment penetrates the ordered and dense crystallites regions appreciably and hydrolyzes the cellulose chain segments causing the degradation and reducing the thermal stability of the compound at the beginning of the process. For samples acetylated for 6 h, we can see the appearing of an exothermic event at 200 °C due to CA crystallization. This suggests the presence of a part of the material that can be crystallized under appropriated conditions and it is a clear indication of a change in the DS value. The 6 h CA showed a broad endothermic event at 223 °C and 273 °C indicating the thermal decomposition of cellulose that had not yet been acetylated. However, the observed endothermic event is broader and shows another peak at 273 °C. For 12 h and 24 h

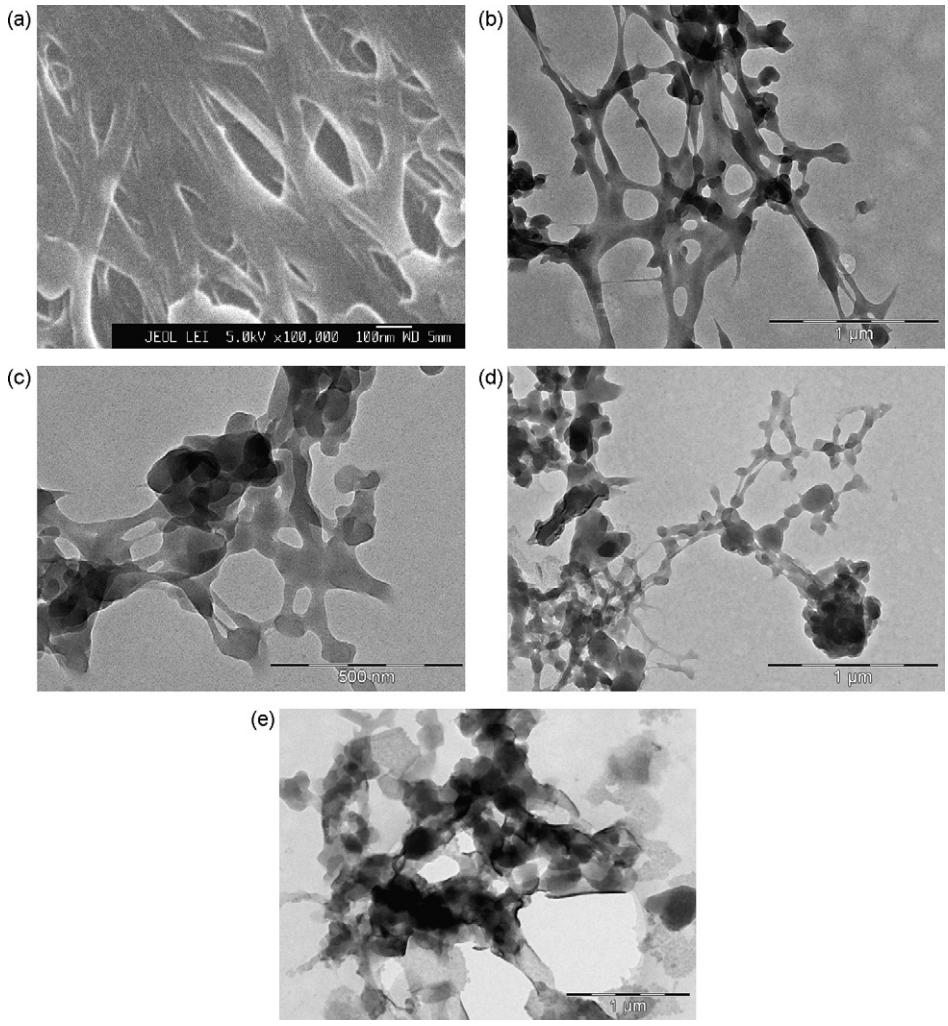

Fig. 5. (a) Scanning electron microscopy of dried BC; and transmission electron microscopy of: (b) CA 1 h; (c) CA 3 h; (d) CA 5 h; (e) CA 24 h.

samples, the evident exothermic peak at 198 °C is due to the crystallization and the endothermic one at around 300 °C is due to melting of the acetylated sample. The fusion temperatures are close to those seen for CTA samples reported in literature [14].

Some aspects seen in the DSC curve can be elucidating by analyzing the TG curves shown in Fig. 7.

The early minor weight loss observed for all samples is attributed to water desorption as was observed in endothermic events (temperature ambient to 100 °C) in the DSC curves. The TG curves revealed the presence of water in all cases, except for samples submitted to a long acetylation time, which showed minor water content. This is principally due to a more substituted material (a greater DS), that is to say, a more hydrophobic material. Bacterial cellulose shows a second event that is attributed to a decomposition process at temperatures higher than 200 °C. The DTG peak (Fig. 8) appears between 205 °C and 398 °C due to a cellulose degradation process such as depolymerization, dehydration, and the decomposition of glucosyl units followed by the formation of a charred residue [15,16].

The CA samples showed different behaviors depending on their acetylation time. The 1 h CA showed a triple-stage decomposition process. The first stage is due to water desorption. The second and third stages are due to polymer decomposition. The aspect of the curve indicates a heterogeneous structure that can be close to bacterial cellulose. The coexistence of microfibers of unmodified cellulose and preacetylated materials is possible. In this condition, the material shows low thermal stability and the decomposition process is more complex due to the presence of acetylated material having a different DS and unmodified cellulose. The events can be better observed in the DTG curve. The DTG peak at 282 °C for the second event can be related with the endothermic peak in the DSC for this sample indicating a degradation process of cellulose acetate produced with 1 h of reaction. This material shows a structure close to bacterial cellulose with a DTG peak of third event at same temperature.

For 6 h CA TG curve shows a curve with more events and worst thermal stability than CA prepared with 1 h of reaction. The increase in the acetylation time improves the acetylation but a more heterogeneous structure is produced. The DTG curve showed two peaks at 190 °C and 337 °C, respectively, which indicates the thermal degradation process. The second event at 190 °C showed a weight loss about 40%. A broad endothermic event at 227 °C is shown in DSC (Fig. 6). This peak is due degradation process that can be seen in TG and due the

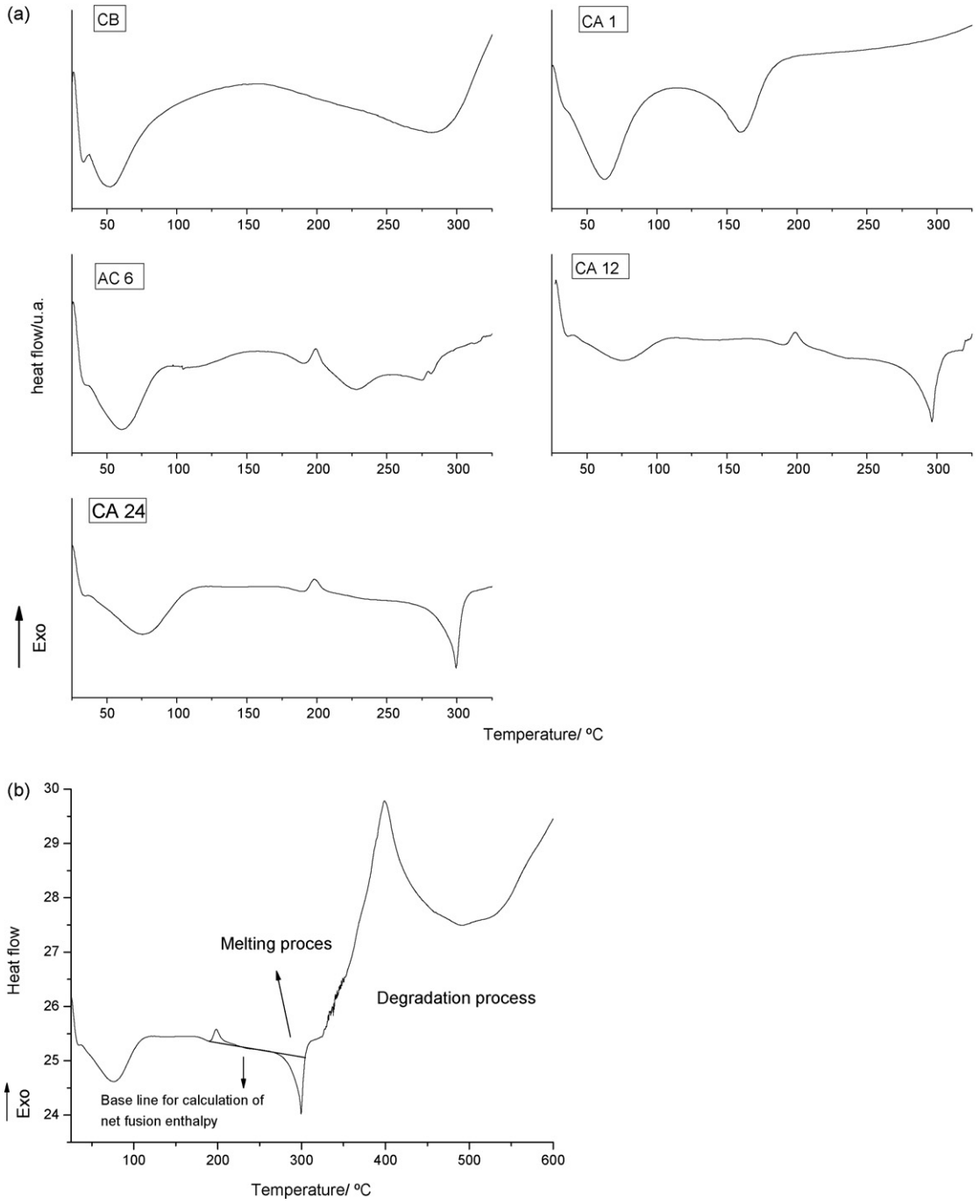

Fig. 6. DSC curves (a) for BC, CA 1 h, CA 6 h, CA 12 h and CA 24 h and (b) representative baseline for enthalpy determination.

heterogeneity of the material is possible that more acetylated portion showed a melting process at 227 °C. This temperature is close to value expected for a cellulose diacetate in literature [14]. According to the DSC curves, this event can be associated to competitive fusion phenomenon of the crystallized material and the degradation of the cellulose derivative.

The TG curves for the 24 h CA showed one main degradation process. A DTG peak between 300 °C and 428 °C appears due depolymerization and pyrolytic decomposition. The 24 h CA shows an improvement in thermal stability in relation to bacterial cellulose and the other CA samples. This material showed a high DS and due the TG and XRD patterns, the structure of the derivative is more homogeneous than other samples prepared using a short acetylation time.

The DSC curves for the CA samples show an endothermic process due to the fusion of the crystalline structure. The existence of crystalline regions in the CA is corroborated by XRD data in Fig. 4. According, Khanna and Kuhn [17], the crystallinity index may be calculated from Eq. (1), in this case, the base line integration peak are put in begin-

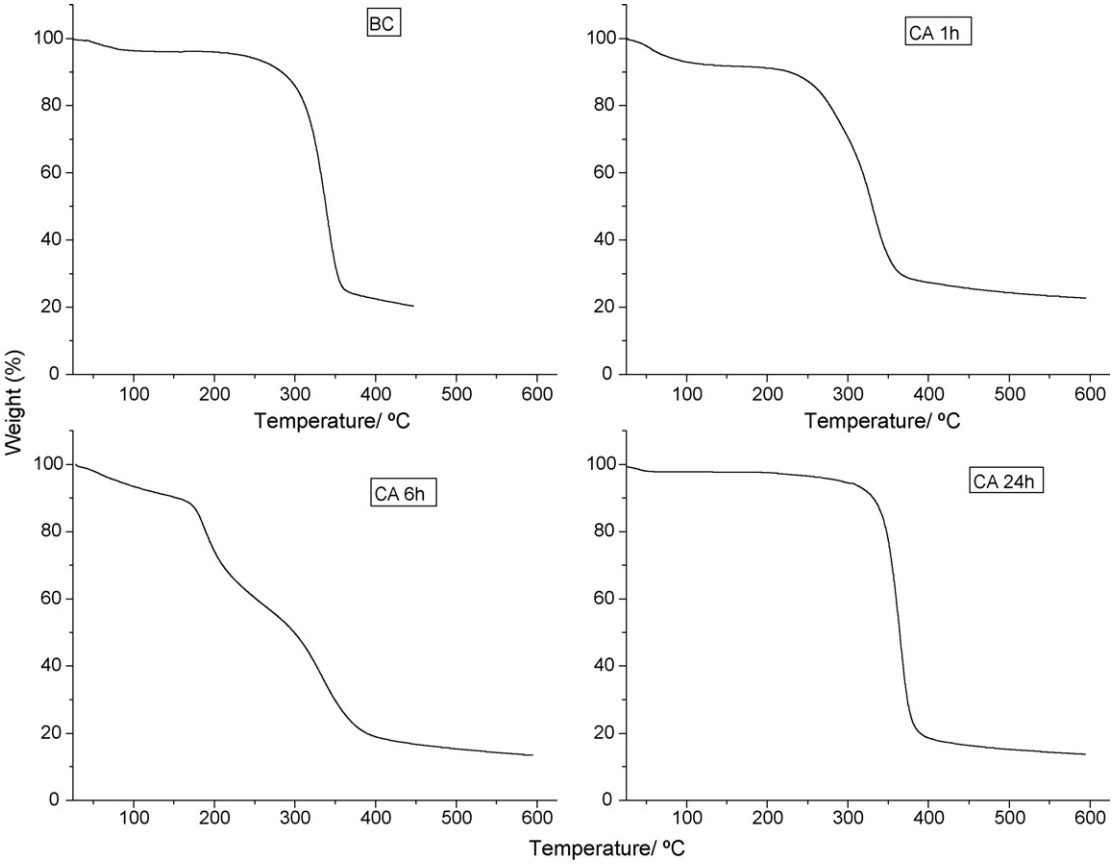

Fig. 7. TG curves for BC, CA 1 h, CA 6 h and CA 24 h.

ning of crystallization process and in the final of melting process. In this case we do not separate integration of the cold crystallization and melting peaks. We take account in a unique calculation the values of crystallization enthalpy, melting enthalpy and silent crystallization. The Fig. 6(b) shows the placement of baseline for crystallinity index (Xc) calculation.

$$\%\mathrm{Xc} = \left(\frac{\Delta H_{\mathrm{fnet}}}{\Delta H_{100\%}}\right) 100 \quad (1)$$

where %Xc is the crystallinity index, ΔH_{fnet} is the cellulose acetate fusion enthalpy net found from the DSC experiment and $\Delta H_{100\%}$ is the fusion enthalpy of perfectly crystalline cellulose triacetate.

Several values have already been proposed for the fusion enthalpy of a perfect crystal of cellulose triacetate. In this work, we have used the value of $58.8\,\mathrm{J\,g^{-1}}$ proposed by Cerqueira et al. [14].

In Fig. 9, it can be observed an increase in the crystallinity index with the time of acetylation, and this value becomes practically constant after 8 h of reaction. For cellulose acetate with a low degree of substitution produced with

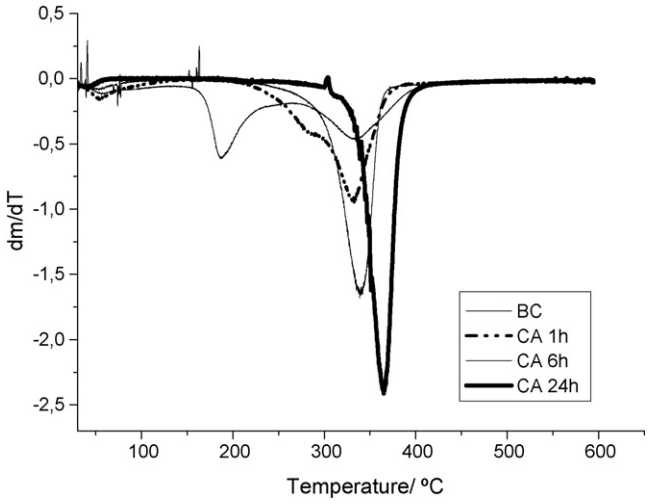

Fig. 8. DTG curves for BC, CA 1 h, CA 6 h and CA 24 h.

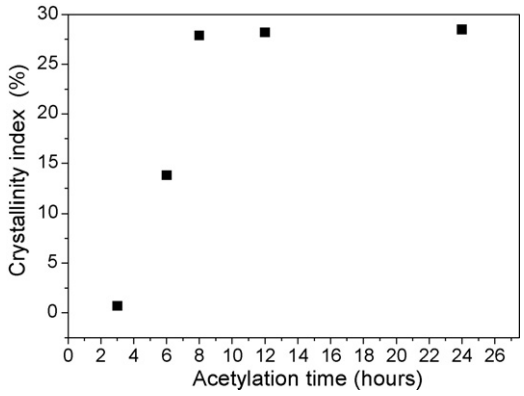

Fig. 9. Crystallinity index (%) versus acetylation time.

0.5–6 h of acetylation, the low crystallinity index is related to random distribution of substitution groups leaving to low chain regularity. For cellulose triacetate produced from 8 h of acetylation, the increase in acetyl groups allow an increase in chain regularity lead to a better chain packing and high crystallinity.

4. Conclusions

Cellulose acetate was produced from the homogeneous acetylation of BC over different lengths times. DS values can be controlled by the acetylation time and this is a very interesting feature, because the production of biodegradable cellulose derivatives is very desirable considering environmental and economic aspects. The characterization of the CA samples acetylated in a shorter time showed the formation of a heterogeneous structure, and in parallel to this, a more homogeneous structure was produced for samples prepared with a longer acetylation time. This fact changes the thermal behavior of the CA samples. Thermal characterization revealed that samples submitted to longer acetylation time's display higher crystallinity and thermal stability than samples submitted to a shorter acetylation time.

Acknowledgements

The authors thank Brazilian agencies FAPESP, CAPES and CNPq for financial support. H.S. Barud, D.A. Cerqueira and C.S. Meireles thank CAPES grants.

The authors would like to thank the LME/LNLS for technical support during electron microscopy work.

References

[1] K.J. Edgar, C.M. Buchanam, J.S. Debenham, J.S. Debenham, et al., Prog. Pol. Deg. 6 (2001) 1605–1688.
[2] G. Rodrigues Filho, S.F. da Cruz, D. Pasquini, D.A. Cerqueira, V.S. Prado, R.M.N. Assunção, J. Membr. Sci. 177 (2000) 225–231.
[3] D. Klemm, B. Heublein, H.-P. Fink, A. Bohn, Angew. Chem. 44 (2005) 3358–3393.
[4] M. Tabuchi, K. Watanabe, Y. Morinaga, F. Yoshinaga, Biosci. Biotechnol. Biochem. 62 (1998) 1451–1454.
[5] D.-Y. Kim, Y. Nishiyama, S. Kuga, Cel 9 (2002) 361–367.
[6] H. Yamamoto, F. Horii, A. Hirai, Cel 13 (2006) 327–342.
[7] J.F. Sassi, H. Chanzy, Cel 2 (1995) 111–127.
[8] E. Samios, R.K. Dart, J.V. Dawkins, Pol 38 (1997) 3045–3054.
[9] R.A. Gross, B. Kalr, Science 297 (2002) 803–807.
[10] D.L. VanderHart, J.A. Hyatt, R.H. Atalla, V.C. Tirumalai, Macromolecules 29 (1996) 730–739.
[11] S. Maunu, T. Litiã, S. Kauliomãki, B. Hortling, J. Sundquist, Cel 7 (2000) 147–159.
[12] M. Wadda, T. Okano, Cel 8 (2001) 173–207.
[13] H.S. Barud, C. Barrios, T. Regiani, M. Verelst, J. Dexpert-Ghys, R.F.C. Marques, Y. Messaddeq, S.J.L. Ribeiro, Mater. Sci. Eng. C 28 (2008) 515–518.
[14] D.A. Cerqueira, G. Rodrigues Filho, R.M.N. Assunção, Pol. Bull. 56 (2006) 475–484.
[15] M. Roman, W.T. Winter, Biomacromolecules 5 (2004) 1671–1677.
[16] H.S. Barud, C.A. Ribeiro, M.S. Crespi, M.A. Martines, J. Dexpert-Ghys, R.F.C. Marques, Y. Messaddeq, S.J.L. Ribeiro, J. Therm. Anal. Calorimetry 87 (2007) 815–818.
[17] Y.P. Khanna, W.P. Kuhn, J. Pol. Sci.: Part B: Pol. Phys. 35 (1997) 2219–2231.